Catalytic Performance and Mechanism of Biomass Tar Reduction: Comparison among Various Carbon-based Catalysts

Supatchaya Konsomboon[1] and Suneerat Fukuda[2*]
King Mongkut's University of Technology Thonburi, 126 Pracha Uthit Road, Bang Mod,
Thung Khru, Bangkok 10140

---

[*] *Corresponding Author: suneerat.pip@kmutt.ac.th*

[1] *Ph.D. Candidate, Energy Technology, The Joint Graduate School of Energy and Environment and Center of Excellence on Energy Technology and Environment.*

[2] *Associate Professor, Head of Advanced Fuel Processing Laboratory (AFPL), The Joint Graduate School of Energy and Environment.*

Article Info

Article History:
Received: May 26, 2023
Revised: October 6, 2023
Accepted: October 12, 2023
DOI: 10.14456/kmuttrd.2023.19

Keywords : Biomass / Tar / Carbon-based Catalyst / Pore Structures / AAEM Species

Abstract

The present study aimed to investigate the performance of carbon-based catalysts and the effect of temperature on decomposition of biomass tar. Three different carbon-based catalysts, i.e., commercial wood biochar (CB char), biochar prepared from slow pyrolysis of eucalyptus wood (EW char), and solid residue from the solvent extraction process of rice straw (RS residue) were tested. Their catalytic activities on the decomposition of naphthalene at 600-800°C were investigated and compared with those in the case of the thermal cracking experiment (without catalyst). Without catalyst, naphthalene conversion was only 25% at 800°C. The presence of catalyst promoted the conversion of naphthalene at all tested temperatures. The highest naphthalene conversion was 72% at 800°C in the presence of CB char. Among the three tested catalysts, CB char was found to have the best catalytic activity for naphthalene conversion due to its larger pore structures; this was followed by EW char and RS residue as the poorest catalyst. Characterization of the catalysts indicated that both pore structure and inherent AAEM species influenced the catalytic activity of carbon-based catalysts. However, the pore structure seem to have more impact on catalytic activity. In all cases, naphthalene decomposition is highly dependent on the temperature. The inherent alkali and alkali earth metallic (AAEM) species, i.e., K and Ca promoted the decomposition of naphthalene, while the presence of Si inhibited the catalytic effect of AAEM species through the formation of alkali silicate.

ประสิทธิภาพและกลไกของตัวเร่งปฏิกิริยาคาร์บอนชนิดต่าง ๆ ต่อการลดการเกิดน้ำมันดินจากชีวมวล

ศุภัชญา คนสมบูรณ์[1] และ สุนีรัตน์ ฟูกุดะ[2*]
มหาวิทยาลัยเทคโนโลยีพระจอมเกล้าธนบุรี 126 ถนนประชาอุทิศ แขวงทุ่งครุ เขตทุ่งครุ กรุงเทพฯ 10140

ข้อมูลบทความ

ประวัติบทความ :
รับเพื่อพิจารณา : 26 พฤษภาคม 2566
แก้ไข : 6 ตุลาคม 2566
ตอบรับ : 12 ตุลาคม 2566
DOI: 10.14456/kmuttrd.2023.19

คำสำคัญ : ชีวมวล / น้ำมันดิน / ตัวเร่งปฏิกิริยาคาร์บอน / โครงสร้างรูพรุน / แร่ธาตุ AAEM

บทคัดย่อ

งานวิจัยนี้ศึกษาประสิทธิภาพของตัวเร่งปฏิกิริยาคาร์บอน 3 ชนิด ได้แก่ ถ่านไม้ชีวภาพที่เตรียมด้วยกระบวนการเชิงพาณิชย์ (CB char) ถ่านชีวภาพจากกระบวนการไพโรไลซิสของไม้ยูคาลิปตัส (EW char) และกากของแข็งที่เหลือจากกระบวนการสกัดฟางข้าวด้วยตัวทำละลาย (RS residue) และผลของอุณหภูมิ (600-800 องศาเซลเซียส) ต่อการสลายตัวของแนฟทาลีน ซึ่งใช้เป็นตัวแทนของน้ำมันดินจากชีวมวล เทียบกับกรณีที่ไม่เติมตัวเร่งปฏิกิริยา ซึ่งพบว่า กรณีที่ไม่เติมตัวเร่งปฏิกิริยา แนฟทาลีนสามารถแปรสภาพได้เพียงร้อยละ 25 ที่ 800 องศาเซลเซียส การเติมตัวเร่งปฏิกิริยาทำให้แนฟทาลีนแปรสภาพเพิ่มขึ้น โดย CB char มีประสิทธิภาพในการแปรสภาพแนฟทาลีนสูงที่สุดถึงร้อยละ 72 ที่ 800 องศาเซลเซียส เนื่องจากสมบัติทางกายภาพของ CB char ที่มีโครงสร้างรูพรุนค่อนข้างใหญ่ รองลงมาคือ EW char ส่วน RS residue มีประสิทธิภาพต่ำที่สุด จากการวิเคราะห์สมบัติของตัวเร่งปฏิกิริยา พบว่าโครงสร้างรูพรุนมีผลต่อประสิทธิภาพในการแปรสภาพแนฟทาลีนมากกว่าแร่ธาตุบนพื้นผิวของตัวเร่งปฏิกิริยา ในทุกกรณี อุณหภูมิยังคงเป็นปัจจัยที่ส่งผลอย่างมากต่อการทำงานของตัวเร่งปฏิกิริยา โลหะอัลคาไลน์และอัลคาไลน์เอิร์ธ (AAEM) ได้แก่โพแทสเซียม (K) และแคลเซียม (Ca) บนพื้นผิวของตัวเร่งปฏิกิริยาช่วยให้เกิดการสลายตัวของแนฟทาลีนได้มากขึ้น ในขณะที่ซิลิกอน (Si) ยับยั้งผลของ AAEM โดยการสร้างสารประกอบอัลคาไลน์ซิลิเกต

---

[*] Corresponding Author: suneerat.pip@kmutt.ac.th

[1] นักศึกษาปริญญาเอก สาขา Energy Technology บัณฑิตวิทยาลัยร่วมด้านพลังงานและสิ่งแวดล้อม และศูนย์ความเป็นเลิศด้านเทคโนโลยีพลังงานและสิ่งแวดล้อม

[2] รองศาสตราจารย์ และหัวหน้าห้องปฏิบัติการ Advanced Fuel Processing บัณฑิตวิทยาลัยร่วมด้านพลังงานและสิ่งแวดล้อม และ ศูนย์ความเป็นเลิศด้านเทคโนโลยีพลังงานและสิ่งแวดล้อม

1. Introduction

Increasing energy demand and attention to global warming has become the driving force to encourage the use of renewable energy resources, which has the benefits of being clean, sustainable, and renewable. Biomass gasification is considered a promising alternative to conventional combustion technology. Differing from combustion, gasification is the conversion of solid fuels by thermochemical process into fuel gases, which is not only used to produce heat and electricity but also for value-added chemicals production. Nevertheless, biomass gasification produced not only useful fuel gases, but also some unwanted by-products. Among them, tar is regarded as one of the most unwanted by-products in gasification process, causing the chemical energy lost, the formation of soot, and a reduction of total energy utilization efficiency in syngas [1]. Moreover, the concentration of tar in biomass gasification is greater than that required by the industry. Syngas containing high tar concentration will affect its application potential.

The development of tar removal technologies has been considered as the important issue to support and develop the efficient gasification process. Tar removal measures can be classified into three approaches, being *i*) thermal cracking *ii*) catalytic cracking *iii*) physical separation. Among these approaches, catalytic cracking is the most promising technique in large-scale processes [2]. One advantage of tar removal by catalytic cracking over thermal cracking is that the heating value of gases is not reduced by cracking of combustible gas components at high temperatures. [3-4]. In addition, the production of usable gases (e.g. H_2 and CO) in producer gas significantly increases.

Several kinds of catalysts have been studied for the removal of tar. Among them, Ni-based catalysts are extensively used for the removal of tar regarding their catalytic activity and economic aspect [3, 5-6]. Nevertheless, the rapid deactivation of Ni-based catalysts from coking leads to its limited lifetime, poisoning and relatively expensive [7]. As the alternative catalyst, carbonaceous materials, i.e. activated carbon and pyrolysis biochar, have been used in the catalytic process as catalyst or catalyst support for tar removal both inside the gasifier and after the product gas leaves the gasifier in the downstream process. The use of carbon-based materials as catalysts is attractive related to its low-cost material, possibility produced from the gasification process, and high poisoning resistance [8]. El-Rub et al. [9] compared the tar removal efficiency using different catalysts and found that biochar can provide high tar conversions as does Ni-based catalysts (>90%).

Literature has found that the catalytic activity of carbon-based materials for the reduction of tar is mainly related to the physical structures (i.e. surface area, pore size and pore volume), as well as the amount and inorganic composition. These are affected by both inherent properties and conditions under which the catalyst is prepared. It has been proven that highly porous chars with inorganic species can provide higher tar conversions [10-11]. Large surface area of carbon-based materials enables the tar adsorption, while pore size and pore volume have an influence on the diffusion rate of gaseous products to react with solid carbonaceous materials [12-13]. The study by Buentello-Montoya et al. [14] showed that the activated biochar offered a higher tar conversion than that of the regular biochar at 650-750°C. Alkali and alkali earth metallic (AAEM) species, e.g. K, Na, Ca and Mg greatly affected the catalytic activity by promoting the condensation reactions of volatile hydrocarbons to form coke

[10, 15]. On the contrary, Si might react with AAEM species, which decreases a catalytic activity due to the availability of the catalytic metals is reduced [16]. These properties result from the difference in feedstock type and the process conditions under which the char is prepared [17-18]. However, there are still limited studies to relate the catalytic activity and the mechanism under which the tar removal occurs considering each dominating property of the carbon-based catalysts.

To investigate the mechanism of tar removal under different influential effects, three biomass-derived carbonaceous materials with different dominating properties were selected for use as the tar removal catalysts. They include commercial wood biochar (i.e. highly porous material), biochar prepared from slow pyrolysis of eucalyptus wood (i.e. low in surface area and porosity as well as inorganic species) and solid residue from the solvent extraction process of rice straw (i.e. rich in inorganic species and comparable pore structure with biochar from eucalyptus wood). All catalysts are produced from or the by-product from processing of biomass which have abundant resource in Thailand. Depending on the nature of tar, the catalytic activity of carbonaceous materials for tar removal is varied. Since tar containing pure aromatic rings are more difficult to convert than tars with heteroatom and aliphatic chains [19], experiments were carried out using naphthalene as the tar model compound. Naphthalene has been widely used as a model tar to investigate the catalytic performance as it is likely the most stable component of biomass tar that difficult to decompose [20, 21]. N_2 atmosphere was used since its major presence (around 55-60% v/v) in producer gas from air-based gasification of biomass. The influence of catalyst bed temperature and characteristics of carbon-based catalysts were investigated with the aim to explore the catalytic performance and possible mechanism governing the tar removal reaction.

2. Materials and methods

2.1 Biochar catalysts

Three different catalysts with different characteristics, i.e. commercial wood biochar (CB char), eucalyptus wood char (EW char), and rice straw residue (RS residue) were applied in this test.

- CB char was wood charcoal supplied from Gammaco Co., Ltd. in a small cube shape with a particle size around 0.5-1 mm.
- EW char was prepared by pyrolyzing eucalyptus wood in a lab-scale fixed bed reactor by heating at 10°C/min under a nitrogen flow and holding at 500°C for 1 h. After that, the sample was cooled down to room temperature before collecting the product biochar.
- RS residue is the by-product from the upgrading process of rice straw by the degradative solvent extraction using 1-methylnaphthalene (1-MN) as a solvent [22]. The solvent extraction was conducting in a high-pressure autoclave reactor by heating up at 5°C/min to 350°C and hold for 60 min. The extracted fraction is carbon-rich and almost ash free, while the unextractable fraction so called residue is enriched with minerals. Since minerals in ash are known to have some catalytic effects for tar cracking, the RS residue which has the ash content as high as 52.2% is likely to have potential as catalyst and therefore chosen for this test.

2.2 Reactor system and test procedures

The catalytic cracking of naphthalene was conducted in a laboratory-scale fixed-bed reactor as presented in Fig. 1. The experimental system comprises of three major parts: *i)* a system for vaporization of naphthalene *ii)* a catalytic fixed-bed reactor and *iii)* a cold tar trap and gas collection unit. The test was carried out using a quartz tube reactor with an inner diameter of 8 mm and 460 mm long. In each experiment, a catalyst with 30 mm bed height was placed on quartz wool at the middle of heating zone inside the reactor. The reactor was heated and controlled by an electrical furnace and the catalyst bed temperature was measured by a K-type thermocouple. Nitrogen was used as the carrier gas and its flow rate was controlled by a mass flow controller. All other parts were also heated externally by the heating tape to avoid condensation of naphthalene vapor and its condensable products. The catalytic cracking experiment was conducted at temperatures ranging from 600°C to 800°C (the typical temperature range for biomass gasification) and held for 100 min at respective temperatures. In each test, nitrogen was purged inside both the fixed-bed reactor and naphthalene vaporization system to remove the remaining oxygen in the system. Then, the reactor was heated to the desired temperature. Naphthalene (99.0% purity, HiMedia) in the reservoir was vaporized at a constant temperature of 150°C. The nitrogen-naphthalene stream and nitrogen were mixed before entering the catalytic reactor at a total flow rate of 100 ml/min, which corresponded to the residence time of 0.1s inside the reaction zone. Once the temperature reached the desired, the naphthalene vapor was fed through the catalytic bed by nitrogen carrier at an average feed rate of 0.03 g/min. The tar collection unit condensed both cracked products and remaining naphthalene, which were subject to the weight and composition analysis. The dry product gas was also collected for composition analysis.

The thermal cracking experiment (without catalyst) was also conducted under the otherwise similar experimental condition for comparison. The blank experiment, i.e. with a catalyst but no naphthalene fed, at corresponding temperatures was also conducted to establish the baseline of gas production from different catalysts, as shown in Fig. 2. Each experiment was repeated at least two times.

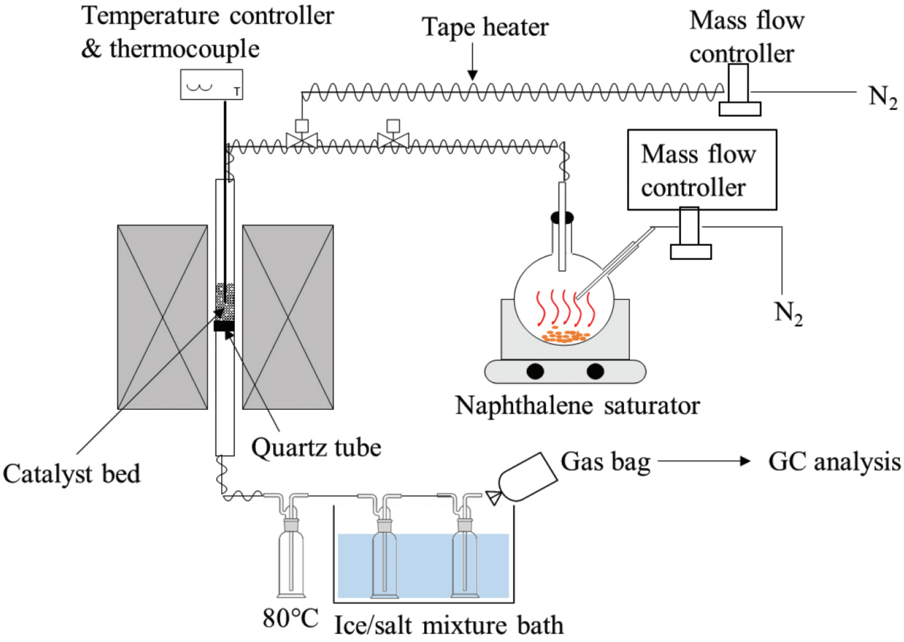

Figure 1 Schematic diagram of catalytic tar removal experiment set up

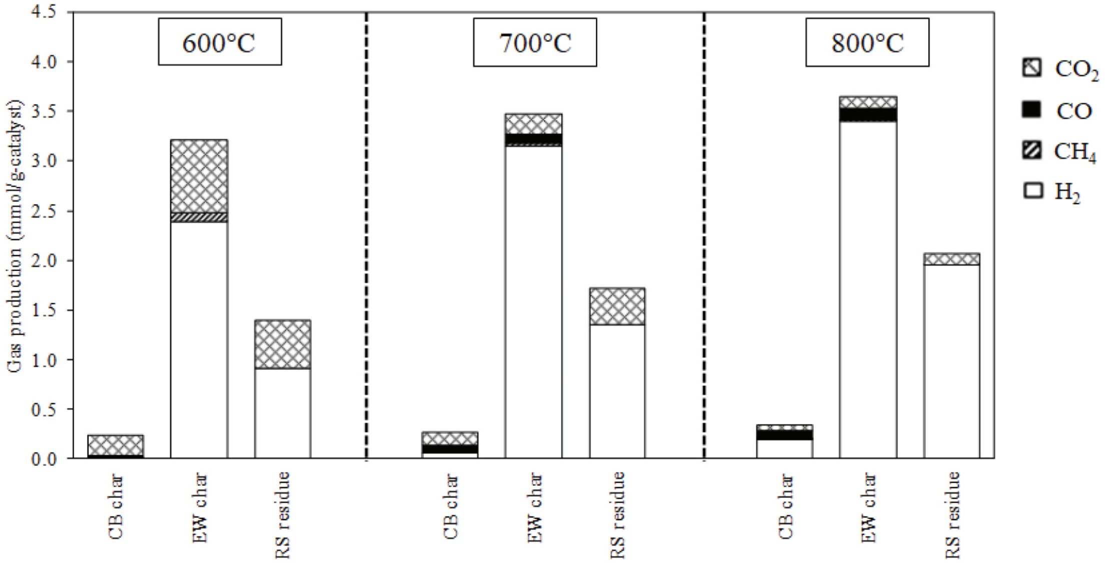

Figure 2 Gas production from blank experiments over different catalysts

2.3 Analytical methods

Tar collection and analysis

All condensable products (or tar) after experiment were collected in the tar collection unit, which comprised a series of three impinge bottles. The first two bottles were filled with isopropanol (IPA) and the remaining one was left empty. The first impinge bottle was externally heated at around 80°C to prevent the condensation of naphthalene vapor and its condensed products. The other two were placed in the cold bath containing ice/salt mixture. Once the experiment was completed, the tar/isopropanol solution from all three bottles were mixed together before further analysis.

The naphthalene content after reaction was quantitatively analyzed by a gas chromatograph (Shimadzu GC2010) with flame ionization detector (FID). The GC column was HP-5 MS column (30 m x 0.25 mm i.d., 0.25 μm film thickness), with flow rate 1.2 mL/min. The temperature of column oven was initially programmed from 45°C (held for 5 min) to 180°C at 5°C/min (held for 5 min), after that ramped from 180°C to 300°C at 20°C/min and held for 20 min at the final step. The naphthalene conversion was calculated from the inlet and outlet amount of naphthalene as presented in Eq. (1)

$$X = \frac{M_{in} - M_{out}}{M_{in}} \times 100 \text{ ----- (Eq. 1)}$$

where X is naphthalene conversion (%), M_{in} is the inlet mass of naphthalene (g) which was calculated from the difference between the weight of naphthalene in the reservoir prior to and after the experiment, M_{out} is the outlet mass of naphthalene (g) or the naphthalene remaining in the tar collection unit after experiment which was determined using GC-FID

Gas analysis

The product gases from the reaction were measured using two models of the gas chromatograph (GC): Shimadzu model GC14B and Shimadzu model GC2014. The content of CO was measured by GC14B through a molecular sieve (MS-5A) column. The contents of H_2, CH_4 and CO_2 were measured by GC2014 equipped with a Pora Plot Q (PPQ) column. Light hydrocarbons heavier than CH_4 were also measured but did not show any significant concentrations

Catalyst characterization

- The proximate analyses was performed by using a thermogravimetric analyzer (TGA) following the standard method of ASTM D5142. The C, H, and N content were determined from the ultimate analysis, while O content was calculated by difference. The major inorganic contents of fresh catalyst were analysed by the Wavelength dispersive X-ray fluorescence spectrometry (WDXRF, Philips model PW2400).
- The surface structures of catalyst was characterized by the gas adsorption technique. The measured properties included surface area, pore volume and mean pore diameter. The surface area and pore volume were measured from the N_2 adsorption-desorption isotherms at -196°C using an automatic volumetric gas adsorption equipment (BELSORP mini II, BEL Japan, Inc.). The Brunauer-Emmet-Teller (BET) calculation method was used to measure the surface area, while the total pore volume was defined as the volume of liquid nitrogen adsorbed at a relative pressure (P/P_0) of 0.99.
- This study focused on alkali and alkali earth metals (AAEMs) and Si, since these elements were present in abundance and likely to have an influence on the catalytic activity during thermal conversion process of solid carbonaceous materials. Due to the limited sample size, the AAEM and Si contents of catalyst from the blank experiment and after the experiment with naphthalene were quantified using the Energy dispersive X-ray spectroscopy (EDS) with the JED-2300 Analysis Station. In each sample, five points were analyzed. The average value of five points was a representative of the AAEM contents on catalyst surface. The carbon content was measured using an elemental analyzer, the same as for the ultimate analysis of fresh catalyst.
- The morphology of the catalyst surface was analyzed by a JEOL JCM-6000 Scanning Electron Microscope (SEM) operated in a High Vacuum (HV) mode.

3. Results and discussion

3.1 Catalyst characteristics

The physical and chemical characteristics of each catalyst including proximate and ultimate analysis, mineral contents, and surface structures are shown in Table 1. For all catalysts, carbon is the main elemental composition with concentration varying around 61-90%. Among the three catalysts, CB char has the lowest H/C and O/C ratios, indicating that CB char was more aromatic and less hydrophilic than others. CB char has relatively large BET surface area and pore volume with the smallest mean pore diameter close to typical values of activated carbon, but the content of minerals especially AAEM species are quite low. In contrast, EW char and RS residue are relatively low in surface area and pore volume with a larger mean pore diameter. K and Ca are the major elements in EW char, while Si is the major element in RS residue.

Table 1 Characteristics of CB char, EW char, and RS residue

	CB char	EW char	RS residue
Proximate analysis (wt.%, dry basis)			
Volatile matter	15.7	33.0	32.9
Fixed carbon	74.8	64.8	14.9
Ash	9.8	2.2	52.2
Ultimate analysis (wt.%, dry ash free basis)			
C	89.8	78.4	61.3
H	0.9	3.2	4.8
N	0.5	0.6	1.1
O	8.8	17.9	32.8
H/C ratio	0.12	0.49	0.94
O/C ratio	0.07	0.17	0.40
AAEM and Si contents (wt.% of catalyst basis)			
K	0.25	1.60	8.34
Ca	0.18	0.21	0.98
Na	0.02	0.00	0.31
Mg	0.14	0.18	1.53
Si	7.10	0.11	37.42
Surface structures			
Surface area (m^2g^{-1})	529.48	2.88	14.28
Pore volume (cm^3g^{-1})	0.31	0.02	0.08
Mean pore diameter (nm)	2.36	23.36	22.41

3.2 Naphthalene feed rate regularity test results

To ensure the accuracy and stability of naphthalene at the inlet throughout the time of the experiment system, the feed rate regularity test was carried out in the same experimental apparatus setup as for the catalytic tar removal experiment (referred to Fig. 1). The temperature was kept at 200°C to avoid any decomposition of naphthalene. The experiment time varied from 0-100 min at 10 min increments. The naphthalene feed rate at each experimental time was calculated from the amount of naphthalene used in the reaction divided by the reaction time. As presented in Fig. 3, the test results show the good credibility with the experimental errors of 0.001 g/min.

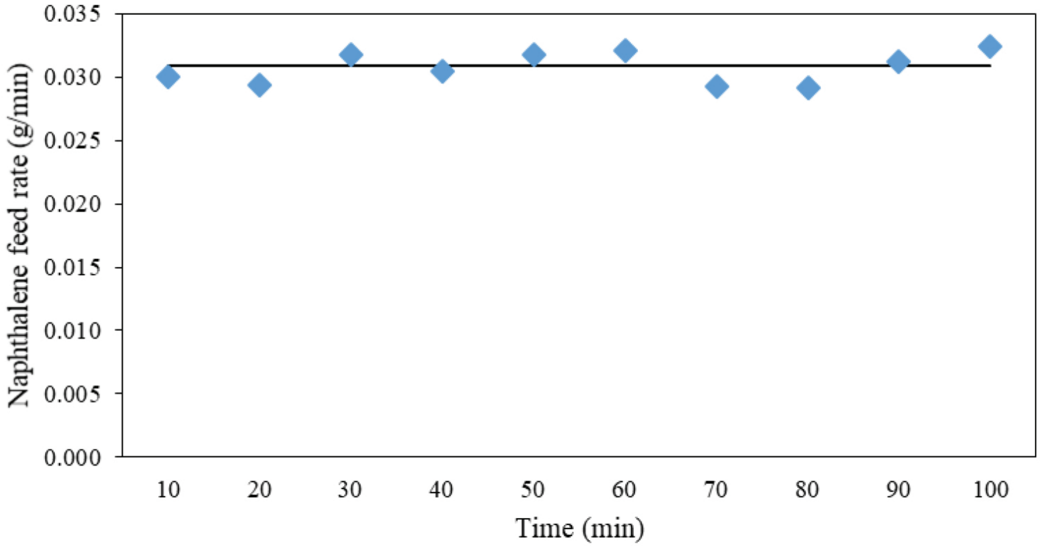

Figure 3 Naphthalene feed rate at the inlet

3.3 Effect of temperatures on naphthalene decomposition over various catalysts

Fig. 4 illustrates the effect of cracking temperature on naphthalene decomposition over three different catalysts, i.e. CB char, EW char and RS residue compared with that from thermal cracking experiment (without catalyst). It is clearly observed that the decomposition of naphthalene increased at high temperature for both thermal cracking and catalytic cracking experiment. However, temperature effects were more pronounced in the presence of catalysts.

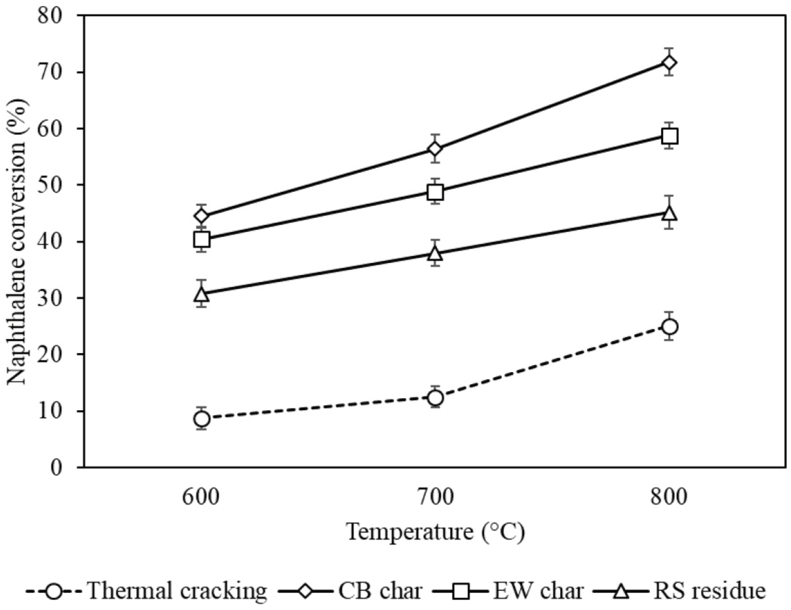

Figure 4 Naphthalene conversion over different catalysts compared with no catalyst addition at 600, 700 and 800°C

Without catalysts, naphthalene remained relatively stable at temperature 600 and 700°C and achieved only 25% conversion at 800°C. With the presence of catalyst, higher naphthalene conversion could be achieved even at 600°C and continued to increase with temperature regardless of catalyst type. Among the three catalysts used, the CB char was found to have the highest catalytic activity for naphthalene conversion, followed by EW char and RS residue as the poorest catalyst. In the presence of CB char, the naphthalene conversion at 800°C achieved almost 72%, compared to around 60% and 45% for EW char and RS residue, respectively. These results show that catalyst characteristics have an influence on naphthalene conversion.

Gas generated as the other product from naphthalene decomposition was also considered. Fig. 5 illustrates the influence of temperature on gas production in the case of CB char, EW char and RS residue compared with that in the case of no catalyst (thermal cracking). As mentioned in Section 2.2, the blank experiment was carried out to establish the baseline in which the gas generated was contributed by the decomposition of the catalyst at corresponding condition. The total gas production was then corrected with the baseline to obtain the net gas production which was contributed by the decomposition of naphthalene only.

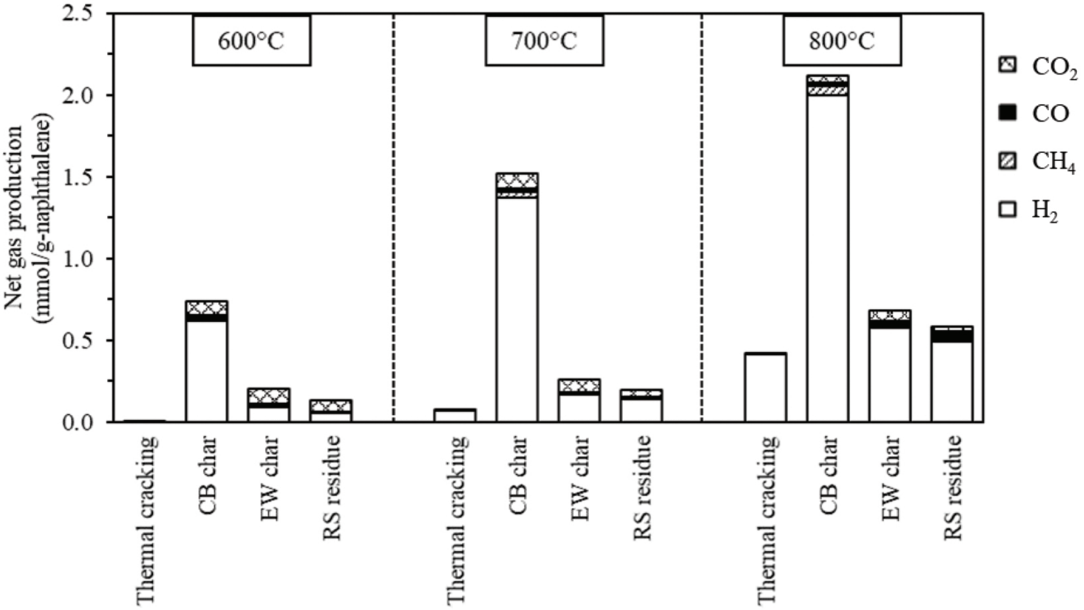

Figure 5 Gas production from naphthalene cracking over different catalysts compared with thermal cracking at various cracking temperatures

In all cases, the increase in temperature gives rise to more gas production. At high temperatures, naphthalene loses its stability and has a greater chance to decompose into smaller compounds and gases. Regardless of the cracking temperature, the presence of all catalysts promoted higher gas yield, as compared to the case of thermal cracking. Thus, all catalysts are likely to play a catalytic role in promoting gas production. For the case of CB char, the gas production consistently increased over the range of temperatures studied, while in the case of thermal cracking, the gas production substantially was promoted at only 800°C. For the case of EW char and RS residue, the gas production also followed the same trend but was unexpectedly low compared to the case of CB char, when considering the increasing trend of naphthalene conversion in Fig. 4. Highest gas production was found in the case of CB chars over the range of temperatures and the gas contained mostly H_2. A large proportion of H_2 probably due to the coke formed onto the large surface of CB char. In the case of thermal cracking, only H_2 with smaller amount of CH_4 were generated. The overall thermal cracking reaction of naphthalene is expressed in (R1). It was reported that the production of H_2 reflects the polymerization reaction of naphthalene [23]. During thermal cracking, H_2 acts as an intermediate for hydrogen transfer, contributing to the decomposition of heavy tar compounds into lighter tar compounds and polymerizing smaller tar compounds into larger tar compounds [24], thus the increased H_2 production can be seen as one of the indicators for naphthalene decomposition.

During catalytic cracking of naphthalene, the products from the thermal cracking of naphthalene came into contact with the catalyst surface and interacted to form H_2, CH_4, CO or CO_2. In this study, different gas formation behaviors were observed, implying that the mechanism of naphthalene decomposition over different catalysts differed. H_2 was found as the main gas species and exhibited the same trend for all catalysts as it increased with increasing temperatures. Since the catalysts used in the test were still thermally active, the condensable products (tar), non-condensable gases (H_2, CH_4, CO, CO_2, C_2) and water were released as a result from the decomposition of catalyst itself, as expressed in (R2). The production of H_2 was then attributed to not only (R1), but also (R3) and (R4). The CH_4 production in the case of CB char and RS residue exhibited the same trend as it increased with temperature, while EW char showed the opposite trend. The increase in CH_4 with increasing temperature was a result from thermal cracking reaction as expressed in (R1), while the lower CH_4 production at higher temperatures was possibly due to the secondary decomposition of tar compounds, which was enhanced at high temperature. The formation of CO and CO_2 were likely attributed to the interactions between oxygen-containing functional groups on catalyst surface and the hydrocarbons molecules derived from thermal cracking of naphthalene cracking (R3) – (R5). For all catalysts, the CO production exhibited the same trend as it increased with increasing temperature, while CO_2 showed the opposite trend. The decrease in CO_2 at higher temperatures was a result from the reaction between the released CO_2 and tar products from thermal cracking (R3) or from (R5), which are favored by the high temperature producing more CO.

$C_{10}H_8 \Sigma \rightarrow C_nH_m + H_2 + CH_4 + C$ ----- (R1)
$C_nH_mO_p \text{ (catalyst)} \rightarrow \text{Tar} + \text{Gases } (H_2, CH_4, CO, CO_2) + H_2O$ ----- (R2)
$C_nH_m + nCO_2 \rightarrow (m/2)H_2 + 2nCO$ ----- (R3)
$C + 2H_2O \rightarrow CO_2 + 2H_2$ ----- (R4)
$C + CO_2 \rightarrow 2CO$ ----- (R5)

Where C_nH_m represents tar compounds from thermal cracking reaction of naphthalene and C represents soot (in a solid form)

The different conversion performances of each catalyst on the decomposition of naphthalene might be attributed to the different characteristics of each catalyst. This assumption was taken into consideration and will be discussed in more details together with the characterization of catalysts before and after the test with naphthalene in the next section.

3.4 Characterization of catalyst before and after the test with naphthalene

3.4.1 Surface structure, weight change and carbon content

The BET surface area and pore volume, catalyst weight change, and carbon content of each catalyst obtained after the experiment with naphthalene at the temperatures in the range of the study against the blank test of catalyst (the case without naphthalene) are shown in Table 2. It was obvious that the BET surface area and the pore volume of catalysts were influenced by temperature. For the catalyst after the blank test, the BET surface area and pore volume increased with increased temperatures due to higher amount of volatile release. However, the maximum BET surface area and pore volume of CB char and RS residue from the blank test were found at 700°C and then decreased as the temperature reached 800°C. The reduction in BET surface area and pore volume of the catalyst at high temperatures resulted from structural ordering and coalescence of micropore from the thermal treatment process [25]. For the used catalyst after the test with naphthalene, the characterization results showed that the BET surface area and pore volume of CB char and RS residue decreased, while EW char exhibited the opposite trend compared with those from the blank test, regardless of the cracking temperatures. The decrease in BET surface area and pore volume of CB char and RS residue is attributed to naphthalene adsorption and soot deposition on the surface of catalyst, which was confirmed by the increased weight and carbon content of those catalysts after the test with naphthalene. According to Hosokai et al. [8], an increased carbon content of catalyst after tar reforming indicated that the deposition rate of tar (to form soot) is greater than the carbon (soot) gasification and vice versa. Therefore, the increased weight and carbon content of CB char and RS residue after the test with naphthalene confirmed that the decomposition of naphthalene in the presence of these catalysts occurred through the adsorption and soot deposition, which is a well-known phenomenon in thermal treatment processes of hydrocarbon especially under reducing atmosphere [26]. As illustrated in Table 2, the BET surface area and pore volume of CB char and RS residue from the blank experiment were found maximum at 700°C, which corresponded to a maximum decrease in BET surface area and pore volume of both catalysts at this temperature. This implies that larger surface area and pore volume of catalysts could adsorb more naphthalene than lower one. In this study, a maximum conversion of naphthalene was found at 800°C for both catalysts (referred to Fig. 4). The lower catalytic activity of CB char and RS residue at 700°C is attributed to the soot deposition on the catalyst surface, which is evidenced by the largest increase in weight and carbon content of catalysts at this temperature. The conversion of naphthalene over both catalysts reached the maximum at 800°C due to enhanced thermal cracking reaction at high temperatures, as seen by increased gas production at this temperature, even with no catalyst present.

In the case of EW char, the increased surface area and pore volume of the catalyst after the test with naphthalene is attributed to the soot gasification of catalyst, which is confirmed by the decreased weight and carbon content of EW char following the catalytic reaction with naphthalene. The decreased carbon content of EW char after tar reforming indicates that the carbon (soot) gasification rate is greater than that of soot deposition. It has been reported previously that the AAEM species, especially K, plays a catalytic role to promote the soot gasification of biochar [27]. Thus, the decrease in carbon content of EW char is possibly attributed to the effect of AAEM species as EW char contains a significant amount of AAEM, especially K. On the contrary, the increased surface area and pore volume of EW char after the test with naphthalene might be related to the activation of EW char by carbondioxide or steam produced during the catalytic process.

Table 2 Characterization results of each catalyst from the blank experiment and after the test with naphthalene at different cracking temperatures

Catalyst	BET surface area (m^2g^{-1})		Pore volume (cm^3g^{-1})		Weight change (%)	Carbon content (%)
	Blank experiment	After test with naphthalene	Blank experiment	After test with naphthalene		
CB char 600°C	609.12	240.56	0.364	0.142	+4.83	+3.24
CB char 700°C	628.75	176.11	0.376	0.112	+14.23	+4.20
CB char 800°C	580.24	264.70	0.353	0.155	+4.74	+2.66
EW char 600°C	2.69	5.46	0.008	0.012	-6.17	-2.32
EW char 700°C	2.85	5.93	0.009	0.015	-7.08	-4.32
EW char 800°C	6.92	18.78	0.021	0.039	-12.34	-4.90
RS residue 600°C	27.11	19.39	0.031	0.017	+16.64	+3.52
RS residue 700°C	35.28	13.34	0.078	0.015	+31.11	+15.16
RS residue 800°C	28.09	16.93	0.057	0.029	+21.21	+18.40

Fig. 6 compares the morphology by SEM analysis of CB char and RS residues obtained from the blank experiment and after the test with naphthalene at 700°C as this temperature might provide the most visible changes owing to the largest difference of catalyst surface area before and after the test with naphthalene. The change in catalyst morphology would allow us to draw a conclusion on the mechanism of naphthalene decomposition over CB char and RS residues. As shown in the SEM images, a remarkable change in CB char and RS residues after the blank experiment and after the test with naphthalene was found. For CB char, the surface morphology of catalyst after blank experiment showed more porosity than the case of catalyst after test with naphthalene. A change in the porous texture of CB char after test with naphthalene was a result of naphthalene adsorption and soot deposition on the surface of CB char [28]. The SEM images of RS residue after blank experiment and after test with naphthalene also showed a clear difference in the surface morphology. After the test with naphthalene, small particles were detected on the RS residue surface. The small particles formed might be the soot deposition as evidenced by the increased carbon content of RS residue after the test with naphthalene.

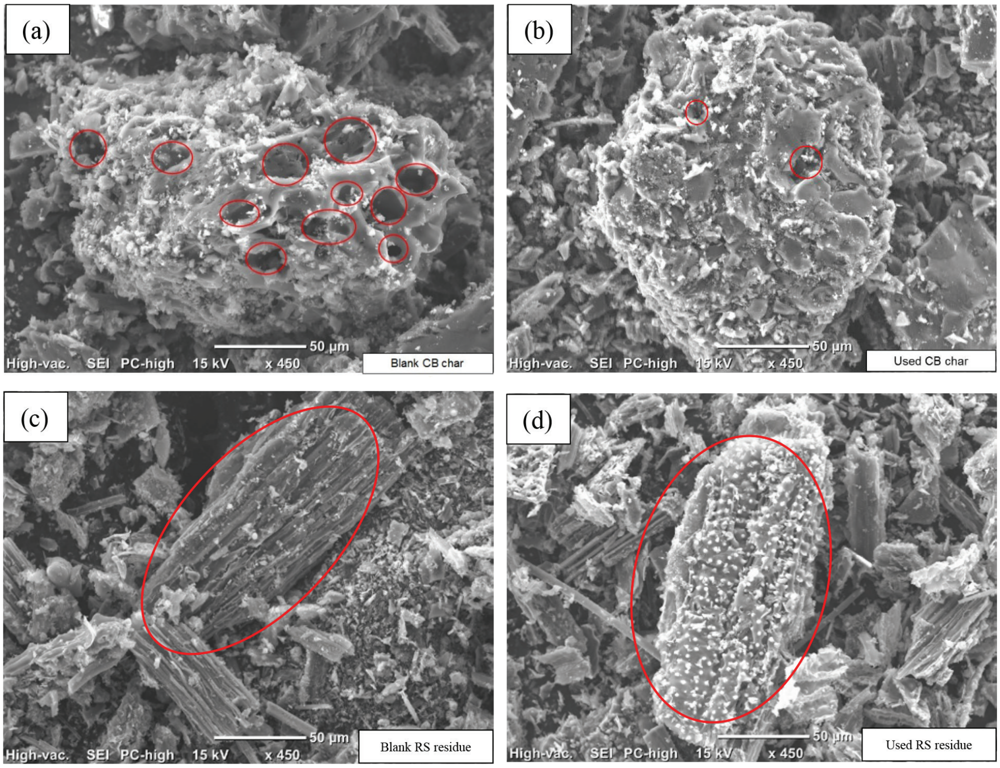

Figure 6 SEM images of the catalyst from the blank test and after the test with naphthalene at 700°C (magnification 450x)

3.4.2 AAEM content

The AAEM species in the carbon-based catalyst may also be released during tar decomposition. In this part, the analysis of AAEM contents in EW char and RS residue was conducted focusing on the effect of K and Ca, which represent the alkali metal and alkali earth metal species, respectively. Since the amount of K and Ca in CB char are relatively low (~ 0.1 wt.%), the influence of K and Ca on naphthalene decomposition in the case of CB char was neglected.

Fig. 7 shows K and Ca retained in EW char and RS residue after blank experiment (no naphthalene feeding) and after the test with naphthalene at different cracking temperatures. In the case of catalyst after blank experiment, similar tendency on the variation of K and Ca was observed for both EW char and RS residue. K and Ca retained in catalyst continuously decreased at elevated temperatures, with reference to the K and Ca content in the fresh catalyst. This confirms that temperature has an impact on the liberation of K and Ca. However, the ratio of K retention was much lower than that of Ca for both catalysts. It was well known that K is released from biomass at the temperature as low as 600°C due to the low melting temperature K compounds was formed [29-30], while Ca compounds may start to release at temperatures above 700°C [27]. The elemental analysis of EW char and RS residue after the test with naphthalene showed that both K and Ca content was lower compared with those from the catalyst after blank experiment. This decrease clearly confirms that K and Ca not only were released from the catalyst by thermal treatment but also took part in promoting the decomposition of naphthalene into H_2 as evidenced by more H_2 in the gas product (referred to Fig. 5). It has previously been reported that K on the char surface is the key component of catalyst for hydrocarbon decomposition, giving the higher yield of H_2, and small molecules of hydrocarbon, like CH_4 [31].

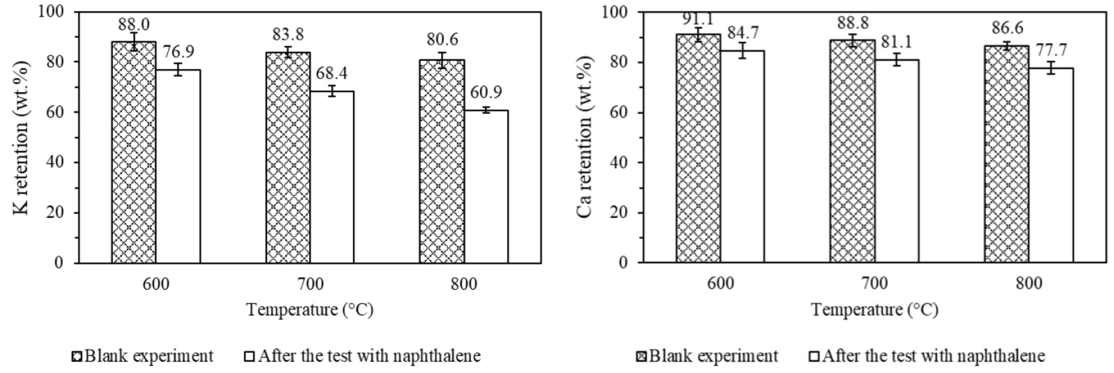

(a) K retained in EW char

(b) Ca retained in EW char

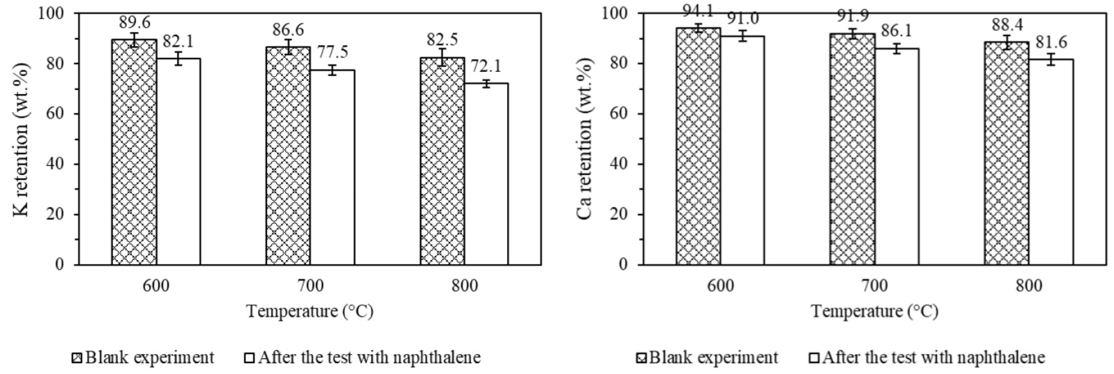

(c) K retained in RS residue

(d) Ca retained in RS residue

Figure 7 Retention of K and Ca (wt.%) in catalyst from the blank experiment and after the test with naphthalene at different cracking temperatures

Generally, K/Ca is directly bonded to the carbonaceous part of catalyst as an intermediate species. The volatilization of K/Ca from the catalyst during catalytic cracking of naphthalene was enhanced by the H radicals generated during the thermal cracking process [32]. The overall reaction for the H radical-induced volatilization and release of K/Ca is expressed in (R6) [33]. During the catalytic process, the H radicals act as intermediate and catalyse K/Ca bonded with the catalyst matrix to the gas phase K/Ca together with the release of Oxygen-containing functional groups, i.e. CO and CO_2 from the carbon matrix of catalyst. The release of K/Ca and Oxygen-containing functional groups to the gas phase resulted in an increase in catalyst active sites. Therefore, it is possible for the volatiles from thermal cracking of naphthalene to bond with or chemisorb on the carbon matrix of catalyst. On the other hand, K/Ca dispersed on the catalyst promotes the formation of coke (soot) through the condensation of volatile hydrocarbons [34]. The radical-induced release of K/Ca is strongly influenced by temperature. As temperature increases, more H radicals and tar fragments were generated, resulting in the more release of K/Ca as presented in Fig. 6, and more catalytic active sites created. Therefore, the possibility of tar molecules to bond with or chemisorb on the carbon matrix of catalyst would increase.

$$K + H = CM\text{-}H + K \text{ ----- (R6)}$$

Where CM and H represent the char matrix and H radicals from thermal cracking of tar, respectively.

From the above results, it can be inferred that the presence of AAEM species especially K promotes the decomposition of naphthalene. In this study, the naphthalene conversion in the case of EW char was much higher than that in the case of RS residue for all cracking temperatures (referred to Fig. 4). The lower naphthalene conversion in the case of RS residue might be attributed to its high Si content. The Si/K ratio of RS residue was 6.25, while that of EW char was only 0.01. At high temperature (~ 800°C), the presence of Si tended to form alkali silicates, which suppressed the effect of AAEM species during the catalytic cracking of tar [16, 27, 35]. This resulted in a lower naphthalene conversion in the case of RS residue as compared with the case of EW char.

3.5 Mechanism of naphthalene decomposition over various catalysts

According to the results of this study, it can be concluded that the catalyst properties, both surface structures (i.e. surface area and pore volume) and the inherent AAEM species in the catalyst influence the decomposition of naphthalene. For the three catalysts used, the possible mechanisms for the decomposition of naphthalene over each catalyst are proposed and summarized as follows:

(a) Naphthalene decomposition over CB char – Due to a large surface area and pore volume of CB char, but limited amount of minerals, the decomposition of naphthalene mainly occurs through the adsorption and soot deposition. During catalytic cracking, naphthalene molecules are adsorbed on the surface area and the pore volume of the catalyst, which acts as active catalyst sites. The adsorbed naphthalene molecules subsequently undergo cracking and polymerization, producing the light hydrocarbons, gases, and soot.

(b) Naphthalene decomposition over EW char – Due to a very low surface area and pore volume, the decomposition of naphthalene over EW char is promoted by the AAEM species, especially K, which acts as catalyst to promote the decomposition of biochar. The free radicals, especially H radicals and active tar fragments generated during the thermal cracking of naphthalene broke the bonds between K and carbon matrix in EW char, leading to the release of K to the gas phase. The volatile K plays a catalytic role by promoting the active sites on the EW char surface where the tar molecules could be bonded with or chemisorb on the carbon matrix of catalyst. In addition, K plays a catalytic role for naphthalene decomposition by promoting the condensation of volatile hydrocarbons to form soot. However, the soot depositing on the surface of EW char is then gasified by CO_2 as evidenced by the increased surface area and pore volume, together with the decreased weight and carbon content of EW char.

(c) Naphthalene decomposition over RS residue - The naphthalene decomposition over RS residue is probably attributed to the combination effects of the surface structures and AAEM species. However, the effect of surface structures is more pronounced compared with the effect of AAEM species. The AAEM species, particularly K, in the RS residue may react with Si to form K-Si, which inhibited the catalytic effect of AAEM species for the tar reduction.

4. Conclusion

The decomposition of naphthalene over three different carbonaceous catalysts, i.e. commercial biochar (CB char), eucalyptus wood char (EW char), and rice straw residue (RS residue) at catalyst bed temperature in the range 600-800°C were examined in a laboratory-scale fixed bed reactor. The results showed that as the temperature was increased, more naphthalene decomposed into gas and other cracking products with or without the presence of catalysts. Thermal cracking of naphthalene could be accelerated only 25% conversion at 800°C. With the presence of catalyst, higher naphthalene conversion could be achieved even at 600°C and continued to increase with increasing temperature. Among three catalysts used, the CB char was found to have the best catalytic performance for naphthalene conversion, followed by EW char and RS residue as the poorest catalyst. The highest naphthalene conversion was 72% at 800°C in the presence of CB char, giving the highest net gas production of about 2.1 mmol/g-naphthalene. Due to the large surface area and pore volume of CB char, adsorption and soot deposition on catalyst surface are the\dominating mechanism for naphthalene decomposition, which led to the deposition of tar to produce coke and H_2. The catalytic activity of EW char and RS residue is lower than that of CB char because the surface area and pore volume are lower. The key performance of EW char and RS residue to promote the decomposition of naphthalene was the AAEM species, especially K and Ca, while the presence of Si inhibited the catalytic effect of AAEM species by the formation of silicates. The results from this study clearly suggest that the larger surface is the more important property to be considered for tar removal catalysts with additional positive effect from the present AAEM species. Further investigation to maximize the surface area of biochar derived from biomass rich in AAEM species and the trial with real product gas from biomass gasification are recommended for the future studies.

5. Acknowledgements

The authors sincerely acknowledge the Thailand Research Fund (TRF) through the Royal Golden Jubilee (RGJ) PhD Program (PHD/0007/2556) and National Research Universities Project (NRU), Thailand's office of the Higher Education Commission and Energy Policy and Planning office (EPPO) for the financial supports.

6. References

1. Wang, G., Xu, S. Wang, C., Zhang, J. and Fang, Z., 2017, "Desulfurization and Tar Reforming of Biogenous Syngas over Ni/Olivine in a Decoupled Dual Loop Gasifier," *International Journal of Hydrogen Energy*, 42 (23), pp. 15471-15478.

2. Shen, Y., Wang, J., Ge, X. and Chen, M., 2016, "By-products Recycling for Syngas Cleanup in Biomass Pyrolysis - An Overview," *Renewable and Sustainable Energy Reviews*, 59, pp. 1264-1268.

3. Yung, M.M., Jablonski, W.S. and Magrini-Bair, K.A., 2009, "Review of Catalytic Conditioning of Biomass-Derived Syngas," *Energy & Fuels*, 23, pp. 1874-1887.

4. Schmidt, S., Giesa, S., Drochner, A. and Vogel, H., 2011, "Catalytic Tar Removal from Bio-Syngas - Catalyst Development and Kinetic Studies," *Catalysis Today*, 175 (1), pp. 442-229.

5. Xiao, X., Liu, J., Gao, A., Zhouya, M., Liu, B., Gao, M., Zhang, X., Lu, Q. and Dong, C., 2018, "The Performance of Nickel-Loaded Lignite Residue for

Steam Reforming of Toluene as the Model Compound of Biomass Gasification Tar," *Journal of the Energy Institute*, 91 (6), pp. 867-876.

6. Kimura, T., Miyazawa, T., Nishikawa, J., Kado, S., Okumura, K., Miyao, T., Naito, S., Kunimori, K. and Tomishige, K., 2006, "Development of Ni Catalysts for Tar Removal by Steam Gasification of Biomass," *Applied Catalysis B: Environmental*, 68 (3-4), pp. 160-170.

7. Li, C., Hirabayashi, D. and Susuki, K., 2009, "Development of New Nickel Based Catalyst for Biomass Tar Steam Reforming Producing H2-Rich Syngas," *Fuel Processing Technology*, 90 (6), pp. 790-796.

8. Hosokai, S., Kumabe, K., Ohshita, M., Norinaga, K., Li, C, and Hayasgi, J., 2008, "Mechanism of Decomposition of Aromatics over Charcoal and Necessary Conditions for Maintaining Its Activity," *Fuel*, 87 (13-14), pp. 2914-2922.

9. Abu El-Rub, Z., Bramer, E.A. and Brem, G., 2008, "Experimental Comparison of Biomass Chars with other Catalysts for Tar Reduction," *Fuel*, 87, pp. 2243-2252.

10. Min, Z., Yimsiri, P., Asadullah, M., Zhang, S. and Li, C-Z., 2011, "Catalytic Reforming of Tar During Gasification. Part II. Char as a Catalyst or as a Catalyst Support for Tar Reforming," *Fuel*, 90 (7), pp. 2545-2552.

11. Song, Y., Wang, Y., Hu, X., Xiang, J., Song, H., Mourant, D., Li, T., Wu, L. and Li, C-Z., 2015, "Effects of Volatile-char Interactions on In-situ Destruction of Nascent Tar during the Pyrolysis and Gasification of Biomass. Part II. Roles of Steam," *Fuel*, 143, pp. 555-562.

12. Mani, S., Kastner, J.R. and Juneja, A., 2013, "Catalytic Decomposition of Toluene Using a Biomass Derived Catalyst," *Fuel Processing Technology*, 114, pp. 118-125.

13. Laurendeau, N., 1978, "Heterogeneous Kinetics of Coal Char Gasification and Combustion," *Progress in Energy and Combustion Science*, 4, pp. 221-270.

14. Buentello-Montoya, D., Zhang, X., Li, J., Ranade, V., Marques, S. and Geron, M., 2020, "Performance of Biochar as a Catalyst for Tar Steam Reforming: Effect of the Porous Structure," *Applied Energy*, 259, 114176.

15. Sun, H., Feng, D., Zhang, Y., Sun, S., Zhao, Y. and Zhang, F., 2022, "Roles of AAEM in Catalytic Reforming of Biomass Pyrolysis Tar and Coke Accumulation Characteristics over Biochar Surface for H2 Production," *International Journal of Hydrogen Energy*, 47 (68), pp. 29207-29218

16. Nzihou, A., Stanmore, B. and Sharrock, P., 2013, "A Review of Catalysts for the Gasification of Biomass Char, with Some Reference to Coal," *Energy*, 58 (1), pp. 305-317.

17. Tripathi, M., Shu, J.N. and Ganesan, P., 2016, "Effect of Process Parameters on Production of Biochar from Biomass Waste through Pyrolysis: A Review," *Renewable and Sustainable Energy Reviews*, 55, pp. 467-481.

18. Li, S., Harris, S., Anandhi, A. and Chen, G., 2019, "Predicting Biochar Properties and Functions Based on Feedstock and Pyrolysis Temperature: A Review and Data Syntheses," *Journal of Cleaner Production*, 215, pp. 890-902.

19. Griffith, D. and Mainhood, J., 1967, "Cracking of Tar Vapour and Aromatic Compounds on Activated Carbon," *Fuel*, 46, pp. 167-176.

20. Coll, R., Salvadó, J., Farriol, X. and Montané, D., 2001, "Steam Reforming Model Compounds of Biomass Gasification Tars: Conversion at Different Operating Conditions and Tendency towards Coke Formation," *Fuel*, 74 (1), pp. 19-31.

21. Xu, C., Donald, J., Byambajav, E. and Ohtsuka, Y., 2010, "Recent Advances in Catalyst for Hot-Gas Removal of Tar and NH3 from Biomass Gasification," *Fuel*, 89 (8), pp. 1784-1795.

22. Jadsadajerm, S., Muangthong-on, T., Wannapeera, J., Ohgaki, H., Miura, K. and Worasuwannarak, N., 2018, "Degradative Solvent Extraction of Biomass Using Petroleum Based Solvents," *Bioresource technology*, 260, pp. 169-176.

23. Zhang, Y., Luo, Y., Wu, W., Zhao, S. and Long, Y., 2014, "Heterogeneous Cracking Reaction of Tar over Biomass Char, Using Naphthalene as Model Biomass Tar," *Energy & Fuels*, 28 (5), pp. 3129-3137.

24. Jess, A., 1996, "Mechanisms and Kinetics of Thermal Reactions of Aromatic Hydrocarbons from Pyrolysis of Solid Fuels," *Fuel*, 75 (12), pp. 1441-1448.

25. Guerrero, M., Ruiz, M.P., Millera, A., Alzueta, M.U. and Bilbao, R., 2008, "Characterization of Biomass Chars Formed under Different Devolatilization Conditions: Difference between Rice Husk and Eucalyptus," *Energy & Fuels*, 22 (2), pp. 1275-1284.

26. Korus, A., Samson, A., Szlek, A., Katelbach-Wozniak, A. and Stadek, S., 2017, "Pyrolytic Toluene Conversion to Benzene and Coke over Activated Carbon in a Fixed-Bed Reactor," *Fuel*, 207, pp. 283-292.

27. Okuno, T., Sonoyama, N., Hayashi, J., Li, C.Z., Sathe, C. and Chiba, T., 2005, "Primary Release of Alkali and Alkali Earth Metallic Species during the Pyrolysis of Pulverized Biomass," *Energy & Fuels*, 19 (5), pp. 2164-2171.

28. Nestler, F., Buehenna, L., Amtenbrink, M.J. and Aicher, T., 2016, "Catalytic Decomposition of Biomass Tars: The Impact of Wood Char Surface Characteristics on the Catalytic Performance for Naphthalene Removal," *Fuel Processing Technology*, 145, pp. 31-41.

29. Jensen, P.A., Frandsen, F.J., Dam-Johansen, K. and Sander, B., 2000, "Experimental Investigation of the Transformation and Release to Gas Phase of Potassium and Chlorine during Straw Pyrolysis," *Energy & fuels*, 14, pp. 1280-1285.

30. Steenari, B-M., Lundberg, A., Petterson, H., Wilewska-Bien, M. and Andersson, D., 2009, "Investigation of Ash Sintering during Combustion of Agricultural Residues and the Effect of Additives," *Energy & Fuels*, 23, pp. 5655-5662.

31. Klinghoffer, N.B., Castaldi, M.J. and Nzihou, A., 2015, "Influence of Char Composition and Inorganics on Catalytic Activity of Char from Biomass Gasification," *Fuel*, 157, pp. 37-47.

32. Gilbert, P., Ryu, C., Sharifi, V. and Swithenback, J., 2009, "Tar Reduction in Pyrolysis Vapours from Biomass over a Hot Char Bed," *Bioresource Technology*, 100 (23), pp. 6045-6051.

33. Hayashi, J.I., Iwatsuki, M., Morishita, K., Tsutsumi, A., Li, C.Z. and Chiba, T., 2002, "Roles of Inherent Metallic Species in Secondary Reactions of Tar and Char during Rapid Pyrolysis of Brown Coals in a Drop-Tube Reactor," *Fuel*, 81 (15), pp. 1977-1987.

34. Wang, F.J., Zhang, S., Chen, Z.D., Liu, C. and Wang, Y.G., 2014, "Tar Reforming Using Char as Catalyst during Pyrolysis and Gasification of Shengli Brown Coal," *Journal of Analytical and Applied Pyrolysis*, 105, pp. 269-275.

35. Dupont, C., Nocquet, T., Da Costa Jr., J.A. and Verne-Tournon, C., 2011, "Kinetic Modelling of Steam Gasification of Various Woody Biomass Chars: Influence of Inorganic Elements," *Bioresource Technology*, 102 (20), pp. 9743-9748.